THE UNIVERSITY OF TEXAS AT AUSTIN

Cockrell School of Engineering

Large Deformation of Hydrogels Coupled with Solvent Diffusion

Rui Huang

Center for Mechanics of Solids, Structures and Materials

Department of Aerospace Engineering and Engineering Mechanics

The University of Texas at Austin

July 2015

Hydrogel = polymer + water (solvent)

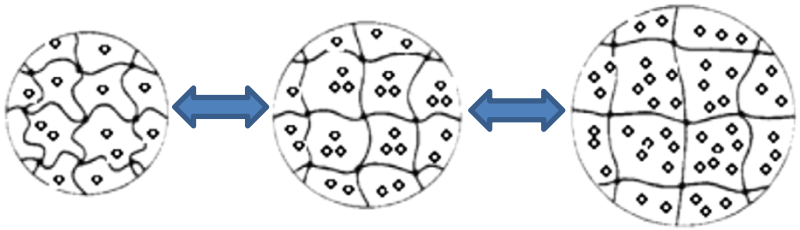

Crosslinked polymer ✚ Solvent molecules

Ambrosio 2010

- Large and reversible deformation facilitated by solvent migration
- Response to mechanical/chemical/electrical stimuli
- Applications: biomedical, soft machines/robots

Transient behaviors of hydrogels

Tanaka et al, 1987

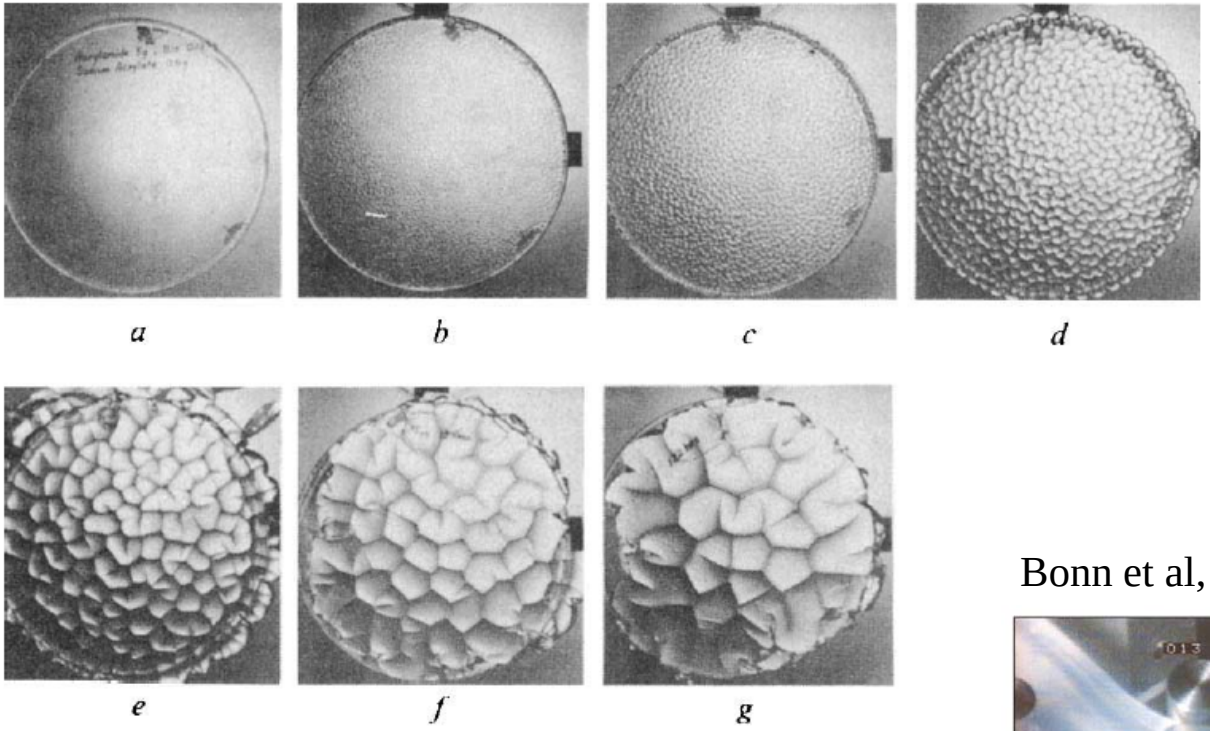

- Swelling
- Indentation
- Fracture
- …

Bonn et al, 1998

Hu et al, 2011

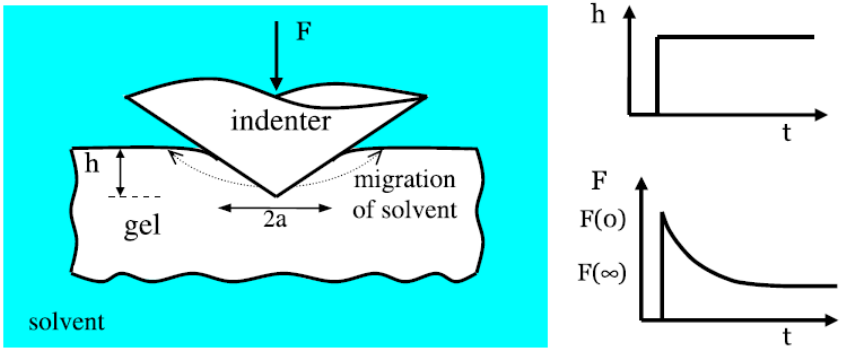

Linear Poroelasticity

$$\frac{\partial \sigma_{ij}}{\partial x_j} + b_i = 0$$

$$\varepsilon_{ij} = \frac{1}{2}\left(\frac{\partial u_i}{\partial x_j} + \frac{\partial u_j}{\partial x_i} \right)$$

- Linear constitutive relation
- Linear kinematics
- Linear kinetics
- Inertia ignored

$$J_k = -\frac{k}{\eta}\frac{\partial p}{\partial x_k}$$

$$\frac{\partial \phi}{\partial t} = \frac{k}{\eta}\frac{\partial^2 p}{\partial x_k \partial x_k}$$

$$\sigma_{ij} = 2G\left[\varepsilon_{ij} + \frac{\nu}{1-2\nu}\varepsilon_{kk}\delta_{ij} \right] - p\delta_{ij}$$

$$\varepsilon_{kk} = \phi - \phi_0$$

3 material parameters: G, ν, k/η

Biot, 1941; Scherer, 1989; Suo et al., 2010.

A Nonlinear Continuum Theory for Gels

Free energy density function: $U(\mathbf{F}, C)$

- Nonlinear constitutive relations
- Nonlinear kinematics
- Geometrically nonlinear kinetics
- Inertia ignored

Nominal stress: $$s_{iK} = \frac{\partial U}{\partial F_{iK}}$$

Chemical potential: $$\mu = \frac{\partial U}{\partial C}$$

Mechanical equilibrium: $$\frac{\partial s_{iK}}{\partial X_K} + B_i = 0$$

Diffusion kinetics: $$J_K = -\frac{DC}{k_B T}\left(\frac{\partial X_K}{\partial x_k}\frac{\partial X_L}{\partial x_k}\right)\frac{\partial \mu}{\partial X_L} = -M_{KL}\frac{\partial \mu}{\partial X_L}$$

Conservation of solvent molecules: $$\frac{\partial C}{\partial t} = -\frac{\partial J_K}{\partial X_K} = \frac{\partial}{\partial X_K}\left(M_{KL}\frac{\partial \mu}{\partial X_L}\right)$$

Hong, Zhao, Zhou, and Suo, 2008.

A Material Model

Flory-Rehner (1943) free energy density function:

$$U(\mathbf{F},C) = U_e(\mathbf{F}) + U_m(C)$$

- Neo-Hookean rubber elasticity:

$$U_e(\mathbf{F}) = \frac{1}{2} N k_B T \left[F_{iK} F_{iK} - 3 - 2\ln\left(\det(\mathbf{F})\right) \right]$$

- Flory-Huggins polymer solution theory:

$$U_m(C) = \frac{k_B T}{\Omega} \left(\Omega C \ln \frac{\Omega C}{1+\Omega C} + \frac{\chi \Omega C}{1+\Omega C} \right)$$

- Volume of gel:

$$\det(\mathbf{F}) = 1 + \Omega C$$

$$U(\mathbf{F},C) = U_e(\mathbf{F}) + U_m(C) + \Pi\left(1 + \Omega C - \det(\mathbf{F})\right)$$

4 material parameters: Nk_BT, $N\Omega$, χ, D

Linearization near a swollen state

Isotropic swollen state: $\lambda_1 = \lambda_2 = \lambda_3 = \lambda_0$

$$\frac{\mu_0}{k_B T} = \ln\frac{\lambda_0^3 - 1}{\lambda_0^3} + \frac{1}{\lambda_0^3} + \frac{\chi}{\lambda_0^6} + N\Omega\left(\frac{1}{\lambda_0} - \frac{1}{\lambda_0^3}\right)$$

$$G = \frac{N k_B T}{\lambda_0}$$

$$\nu = \frac{1}{2} - \frac{N\Omega}{2}\left[\frac{1}{\lambda_0^2(\lambda_0^3 - 1)} + \frac{N\Omega}{\lambda_0^2} - \frac{2\chi}{\lambda_0^5}\right]^{-1}$$

$$M_0 = \frac{D}{\Omega k_B T}\frac{\lambda_0^3 - 1}{\lambda_0^3}$$

$$\sigma_{ij} = 2G\left[\varepsilon_{ij} + \frac{\nu}{1-2\nu}\varepsilon_{kk}\delta_{ij}\right] - \frac{\mu - \mu_0}{\Omega}\delta_{ij}$$

$$j_k = -\frac{c_0 D}{k_B T}\frac{\partial \mu}{\partial x_k} = -M_0\frac{\partial \mu}{\partial x_k}$$

$$\frac{\partial c}{\partial t} = -\frac{\partial j_k}{\partial x_k} = M_0\frac{\partial^2 \mu}{\partial x_k \partial x_k}$$

$$\varepsilon_{kk} = \Omega(c - c_0) \qquad \Omega c_0 = 1 - \lambda_0^{-3}$$

- The linearized equations are identical to the theory of linear poroelasticity.
- The 3 parameters in the linearized equations depend on the swelling ratio.

$$p \Leftrightarrow \frac{\mu - \mu_0}{\Omega} \qquad \phi \Leftrightarrow \Omega c \qquad \frac{k}{\eta} \Leftrightarrow \frac{D}{k_B T}\frac{\lambda_0^3 - 1}{\lambda_0^3}$$

Bouklas and Huang, Soft Matter 2012.

Poisson's ratio

Yoon et al., Soft Matter 6, 6004-6012 (2010).

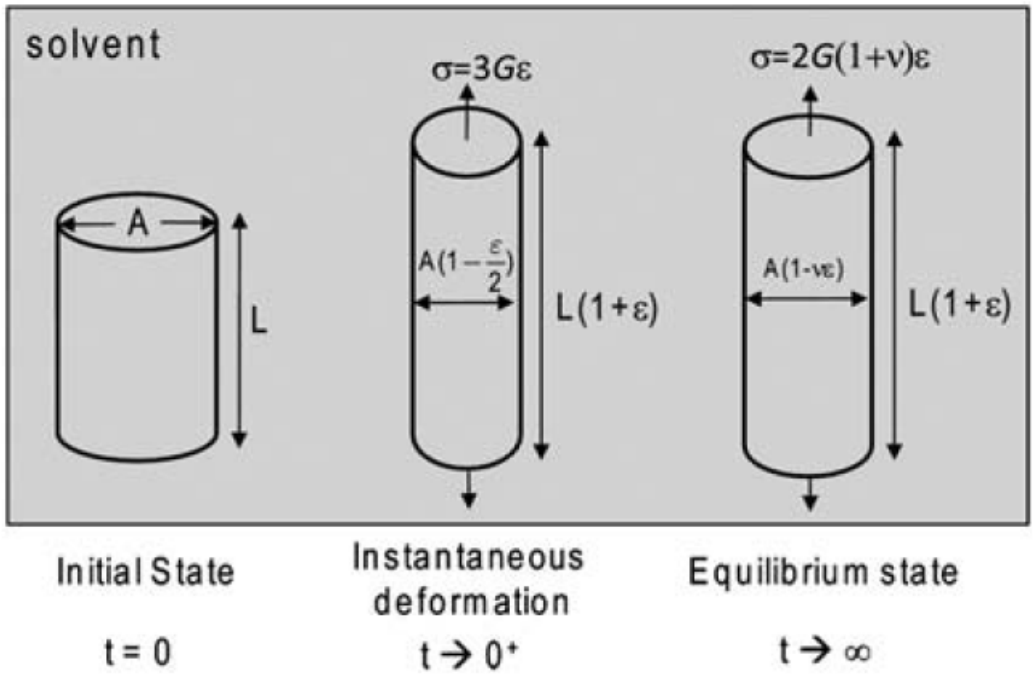

$$\nu = \frac{1}{2} - \frac{N\Omega}{2}\left[\frac{1}{\lambda_0^2(\lambda_0^3-1)} + \frac{N\Omega}{\lambda_0^2} - \frac{2\chi}{\lambda_0^5}\right]^{-1}$$

- Instantaneously incompressible ($\nu_0 = 0.5$)
- The equilibrium Poisson's ratio depends on the initial state (λ_0 or μ_0) as well as the intrinsic material properties (χ and $N\Omega$).

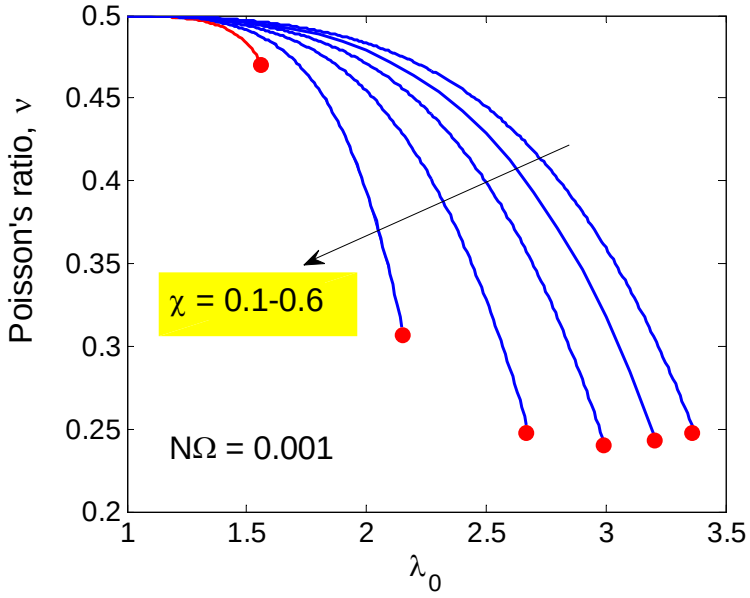

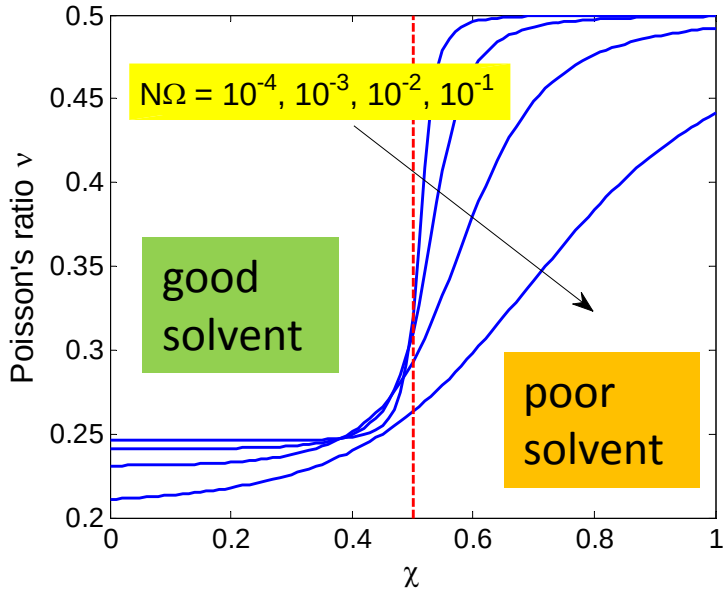

Bouklas and Huang, Soft Matter 2012.

A nonlinear, transient finite element method

Weak form for the coupled fields:

$$\int_{V_0}\left(s_{iJ}\delta u_{i,J} - C\delta\mu + \Delta t J_K \delta\mu_{,K}\right)dV = \int_{V_0}\left(b_i\delta u_i - r\Delta t\delta\mu - C^t\delta\mu\right)dV + \int_{S_0} T_i\delta u_i dS - \int_{S_0} i\Delta t\delta\mu dS$$

Discretization

$$\mathbf{u} = \mathbf{N}^u\mathbf{u}^n \qquad \boldsymbol{\delta}\mathbf{u} = \mathbf{N}^u\boldsymbol{\delta}\mathbf{u}^n$$

$$\mu = \mathbf{N}^\mu\boldsymbol{\mu}^n \qquad \delta\mu = \mathbf{N}^\mu\boldsymbol{\delta}\boldsymbol{\mu}^n$$

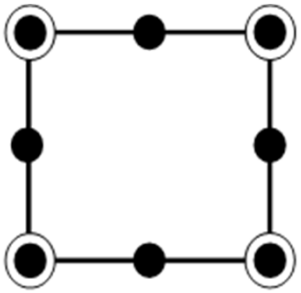

- For numerical stability, the 2D Taylor-Hood elements (8u4p) are implemented.

A slightly different material model:

$$U(\mathbf{F},C) = U_e(\mathbf{F}) + U_m(C) + U_c(F,C)$$

$$U_c(\mathbf{F},C) = K\frac{\left(\det(\mathbf{F}) - 1 - \Omega C\right)^2}{2}$$

Legendre transform

$$\hat{U}(\mathbf{F},\mu) = U(\mathbf{F},C) - \mu C$$

Bouklas et al., JMPS 2015

Numerical stability for mixed finite element method

- Nearly incompressible behavior at the instantaneous response limit $t \longrightarrow 0$ for $K >> Nk_BT$
- Discontinuity of the boundary condition at $t = 0^+$ with respect to the initial conditions

Choice of appropriate interpolations:

LBB condition (Ladyzhenskaya-Babuska-Brezzi)

Displacement node

Chemical potential node

UNSTABLE

Equal order

8u8p

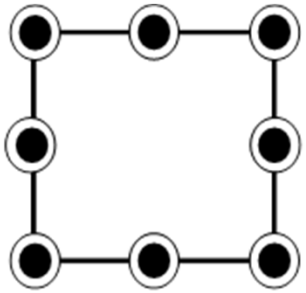

STABLE

Taylor Hood

8u4p

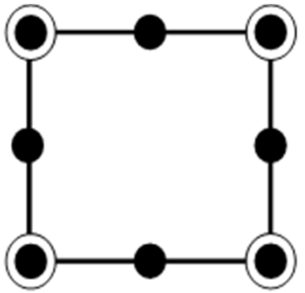

- **Incompressible linear elasticity**
- **Stokes flow**
- **Linear poroelasticity**

Constrained swelling of hydrogel layers

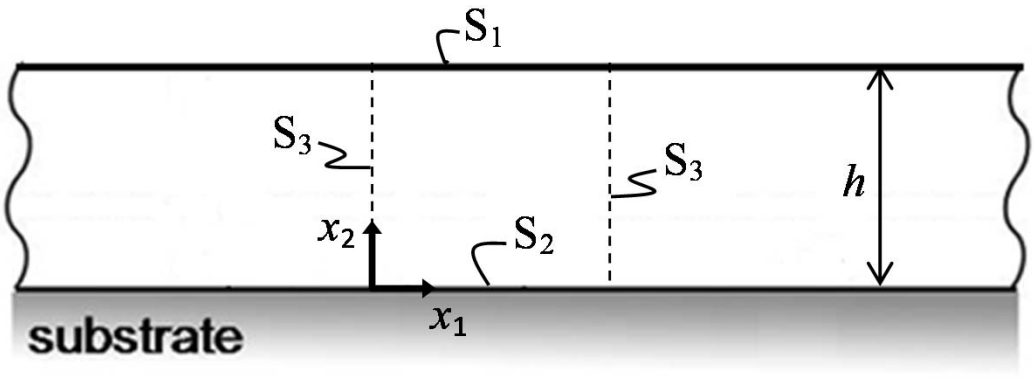

IC's

$$\mathbf{u}(\mathbf{X},0) = \lambda_0 \mathbf{X} - \mathbf{X}$$

$$\mu(\mathbf{X},0) = \mu_0$$

BC's

$$S_1 : \mu = 0$$
$$S_2 : \Delta\mathbf{u} = \mathbf{0}, J_2 = 0$$
$$S_3 : \Delta u_1 = 0, J_1 = 0$$

UNSTABLE

Equal order

8u8μ element

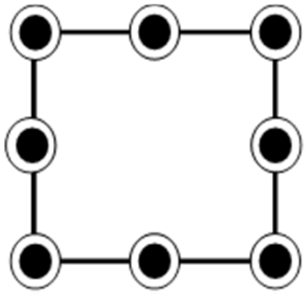

Oscillations in the early stage

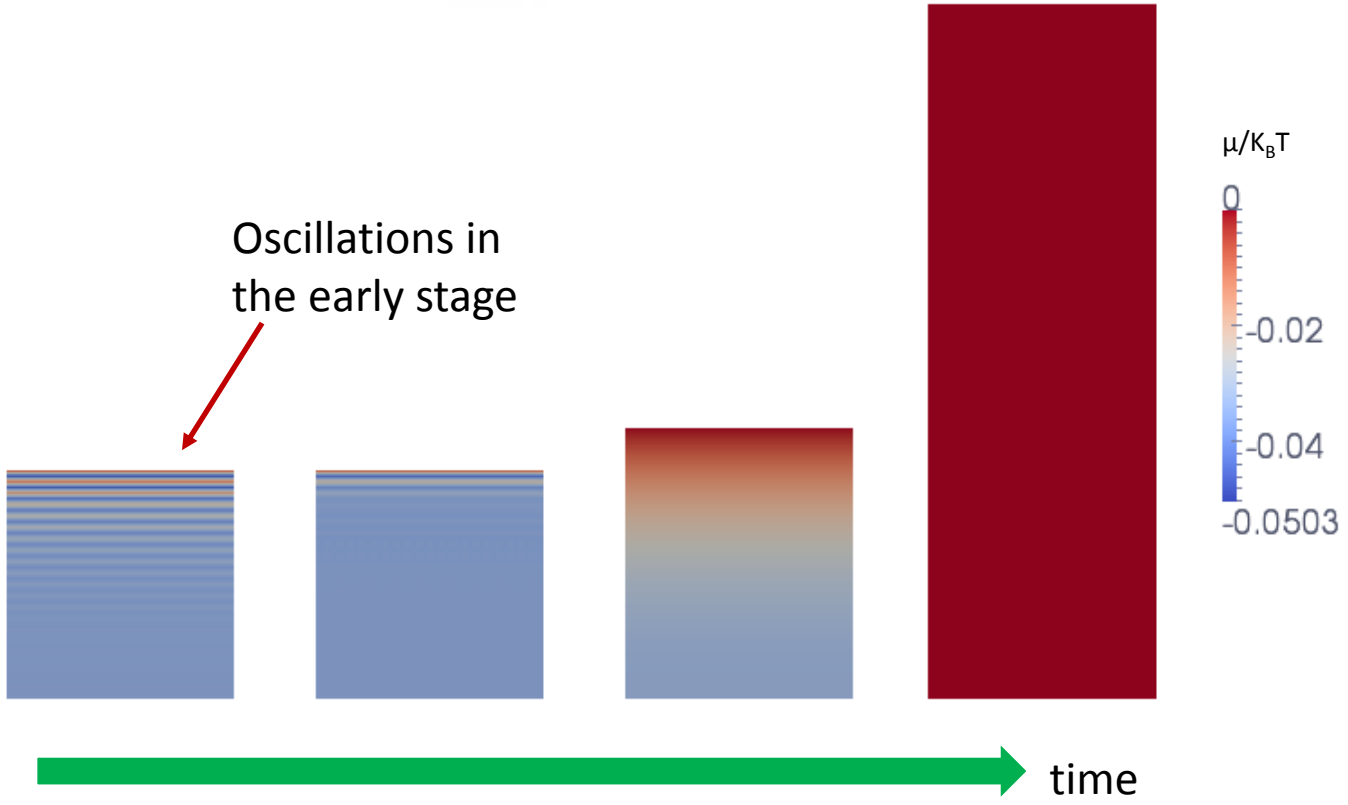

Evolution of chemical potential oscillations

UNSTABLE

8u8μ

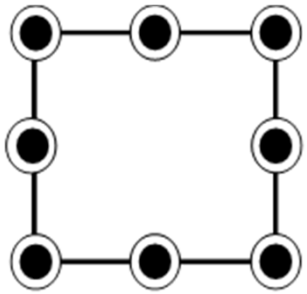

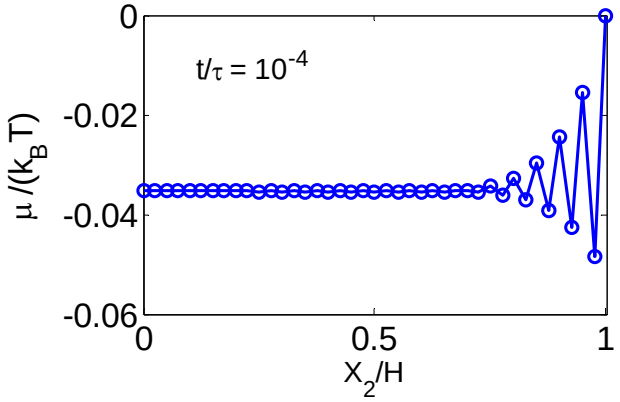

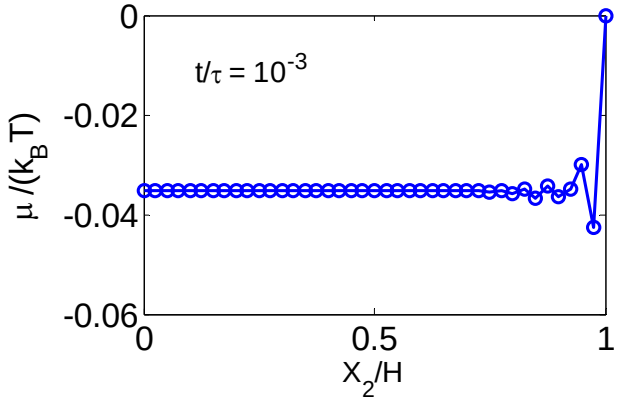

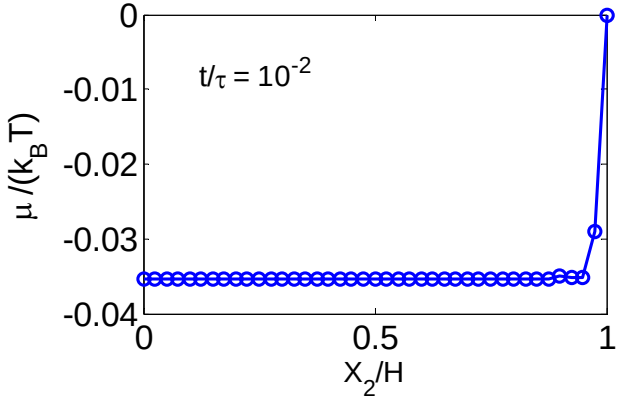

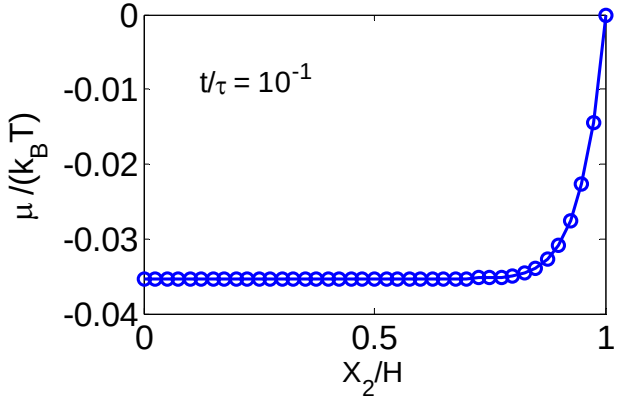

$$\tau = \frac{H^2}{D}$$

$$\lambda_0 = 1.4, N\Omega = 0.001$$

$$\chi = 0.4, K = 10^3 N k_B T$$

Effect of compressibility

UNSTABLE

8u8μ

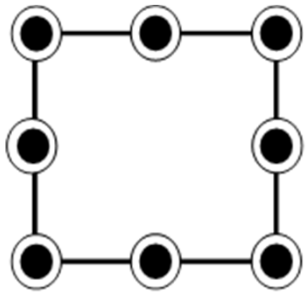

$\lambda_0 = 1.4, N\Omega = 0.001$

$\chi = 0.4$

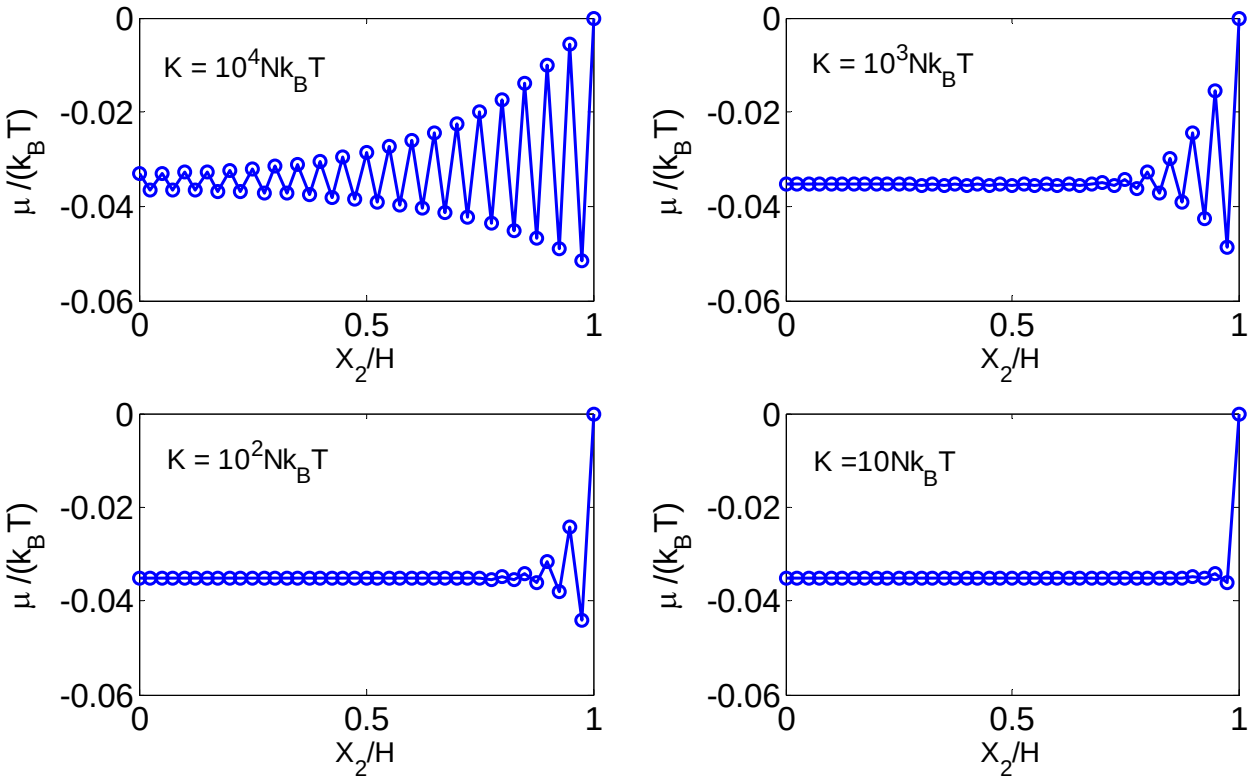

$t / \tau = 10^{-4}$

The oscillations decrease with increasing compressibility (K decreasing)

Use of stable interpolation

STABLE

Taylor Hood

8u4μ element

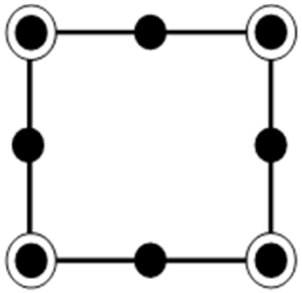

$\lambda_0 = 1.4, N\Omega = 0.001$

$\chi = 0.4, K = 10^3 Nk_B T$

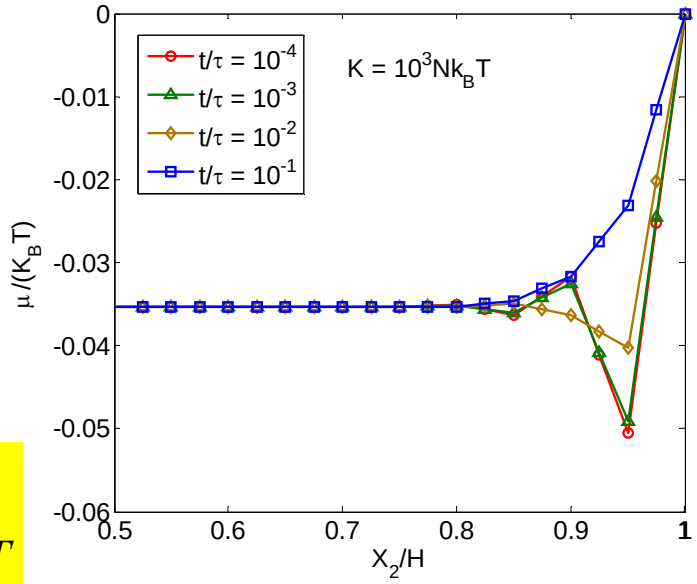

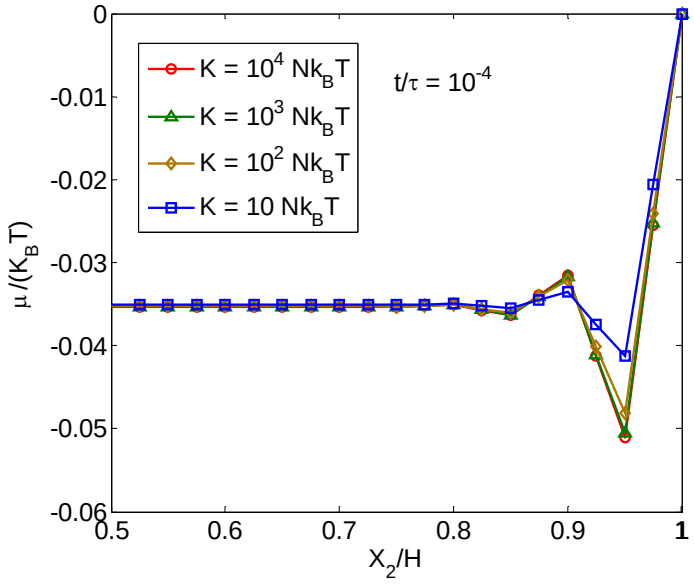

- Oscillations are significantly reduced and do not depend on compressibility.
- The remaining oscillations are due to discontinuity of the boundary condition at $t = 0^+$.

Bouklas et al., JMPS 2015

Swelling induced surface instability

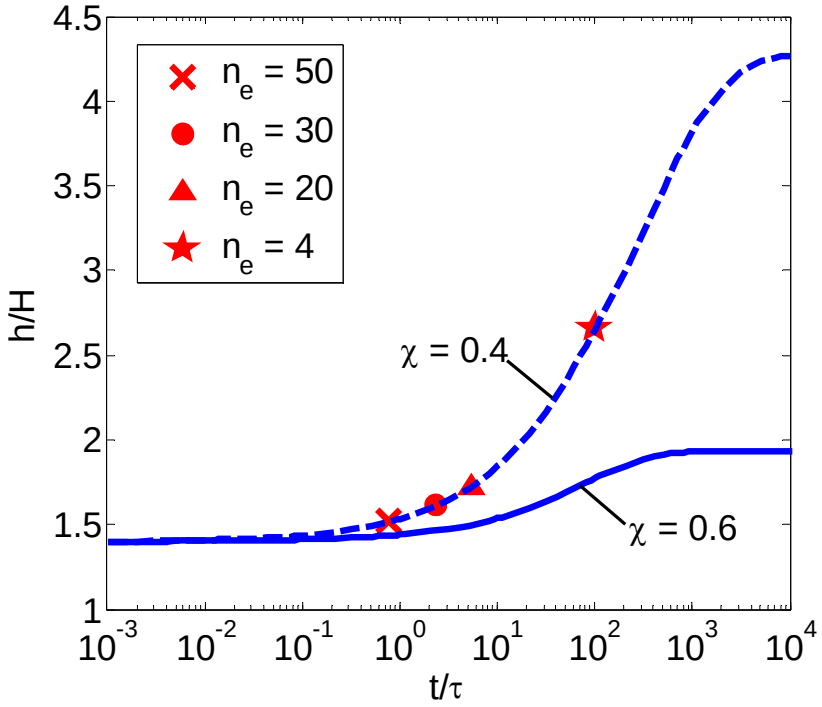

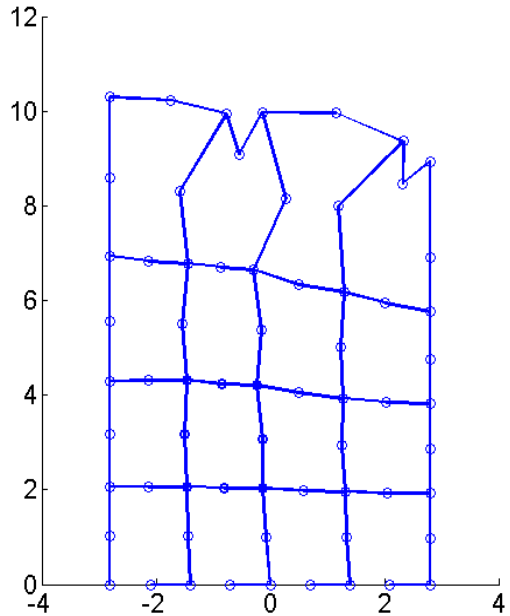

- Swell induced compressive stress could lead to surface instability
- For a poor solvent (χ = 0.6), the surface remains flat and stable.
- For a good solvent (χ = 0.4), the homogeneous hydrogel layer is instantaneously unstable upon swelling; numerically, divergence occurs at a finite time that depends on the mesh size.

Bouklas et al., JMPS 2015

Swell induced surface wrinkling

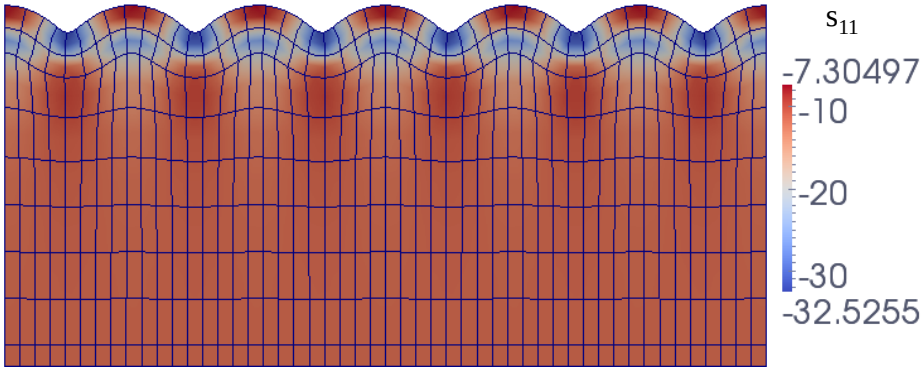

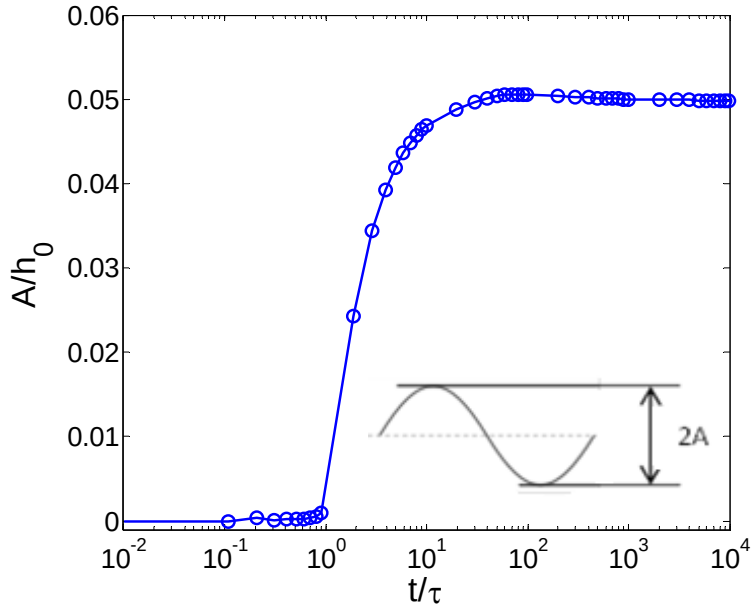

- Regularization of the surface instability by using a stiff skin layer.
- Wrinkle amplitude grows over time, with a selected wrinkle wavelength.

Bouklas et al., JMPS 2015

Two types of surface instability

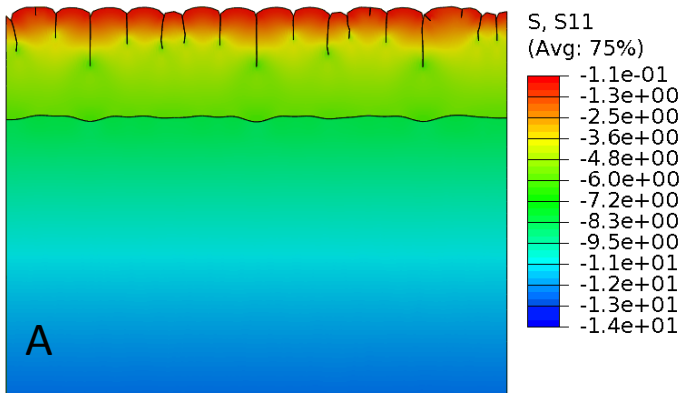

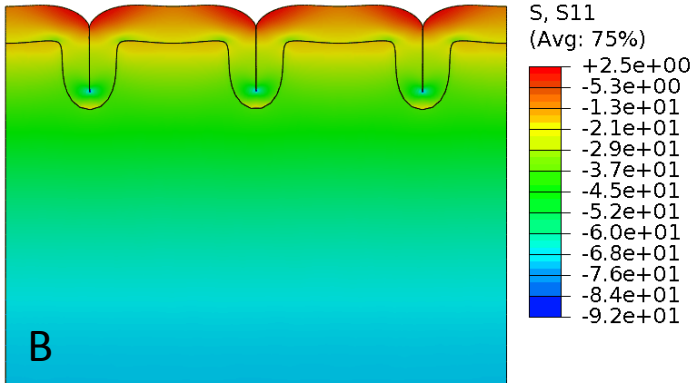

- **Type A:** soft-on-hard bilayer, critical condition at the short wave limit, forming surface creases;
- **Type B:** hard-on-soft bilayer, critical condition at a finite wavelength, forming surface wrinkles first.

Wu, Bouklas and Huang, IJSS 50, 578-587 (2013).

A soft-on-hard gel bilayer (Type A)

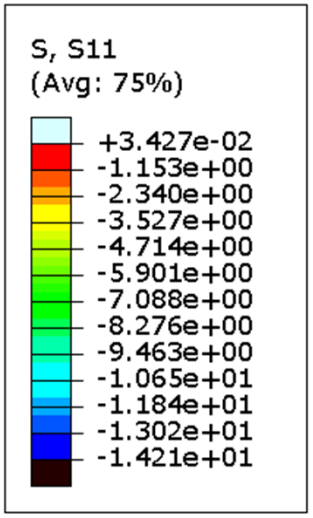

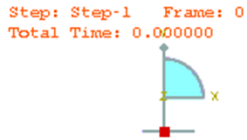

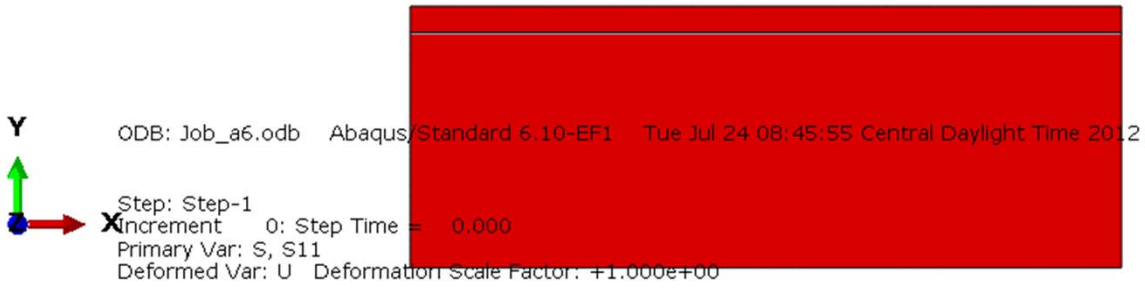

A hard-on-soft gel bilayer (Type B)

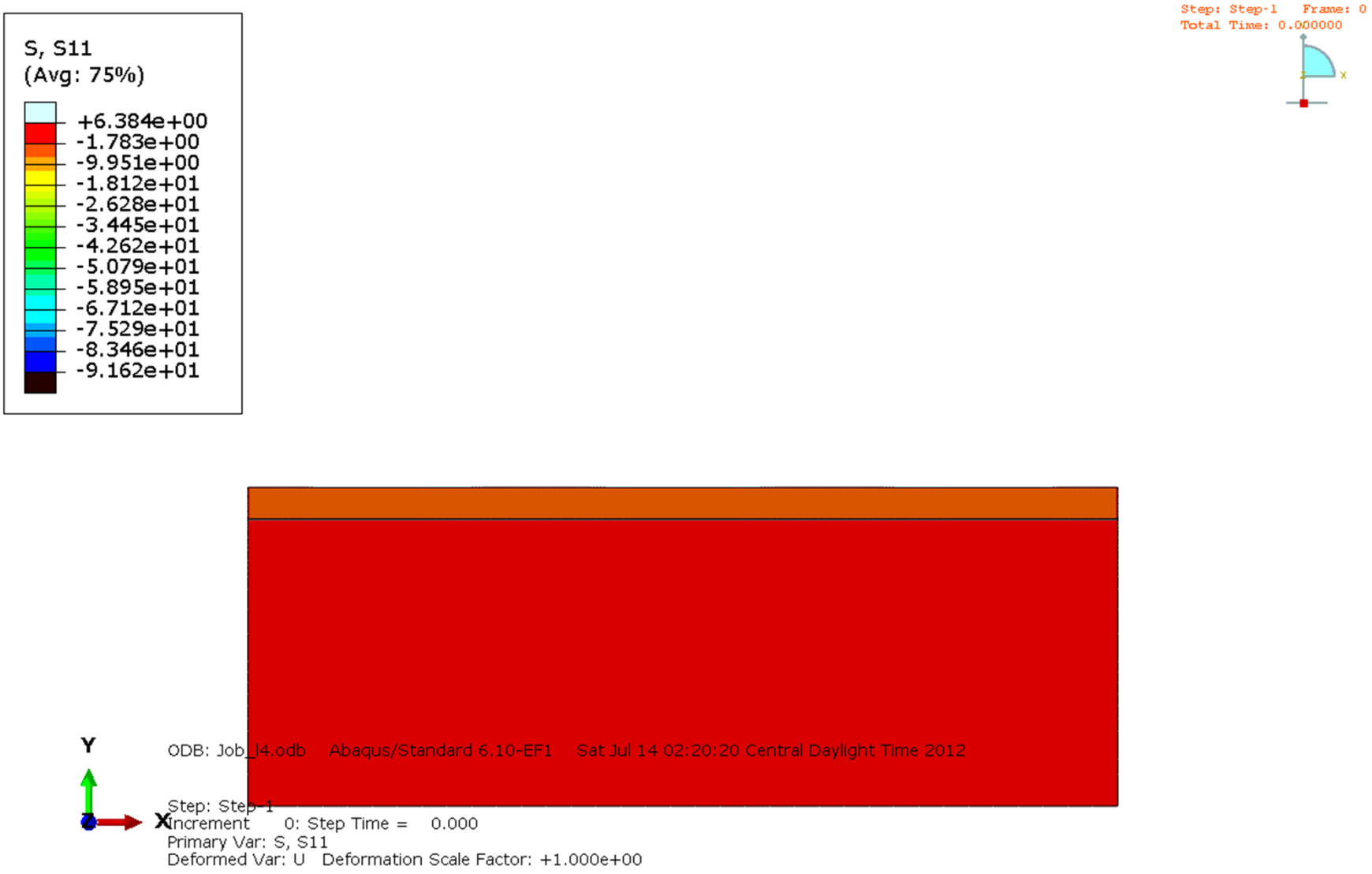

Flat Punch Indentation

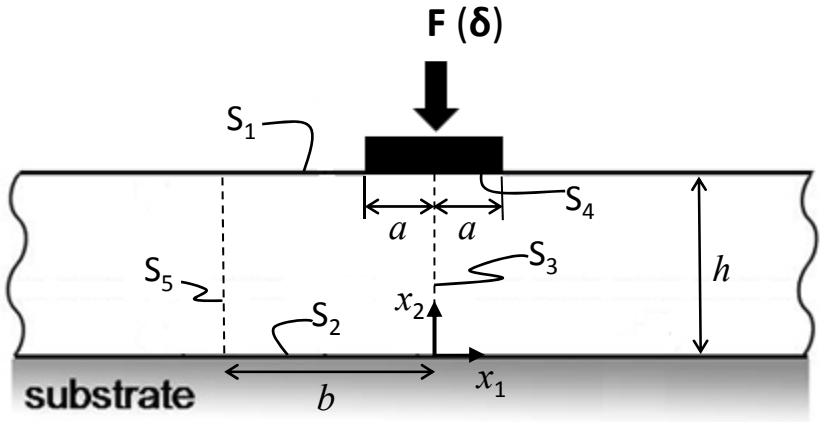

$$\overline{F}(t) = (F(t) - F(\infty)) / (F(0) - F(\infty))$$

$$\tau = \frac{\alpha^2}{D}$$

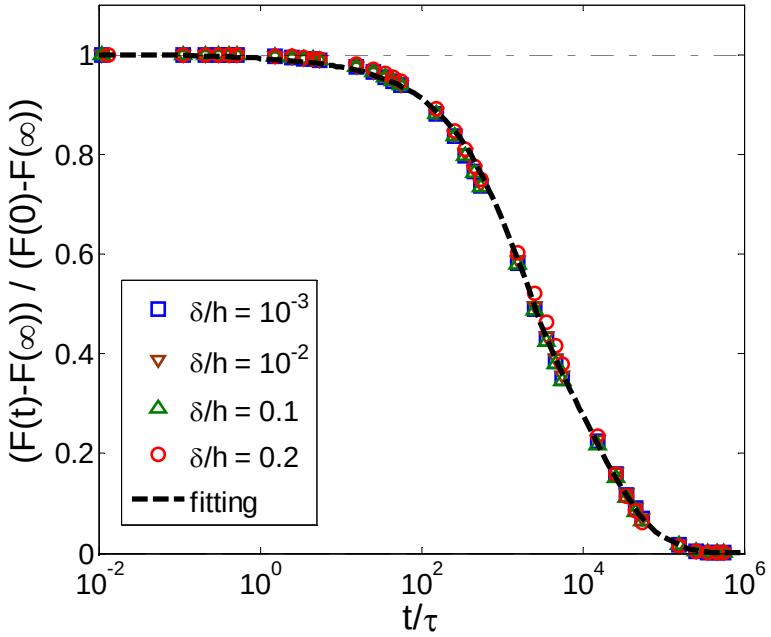

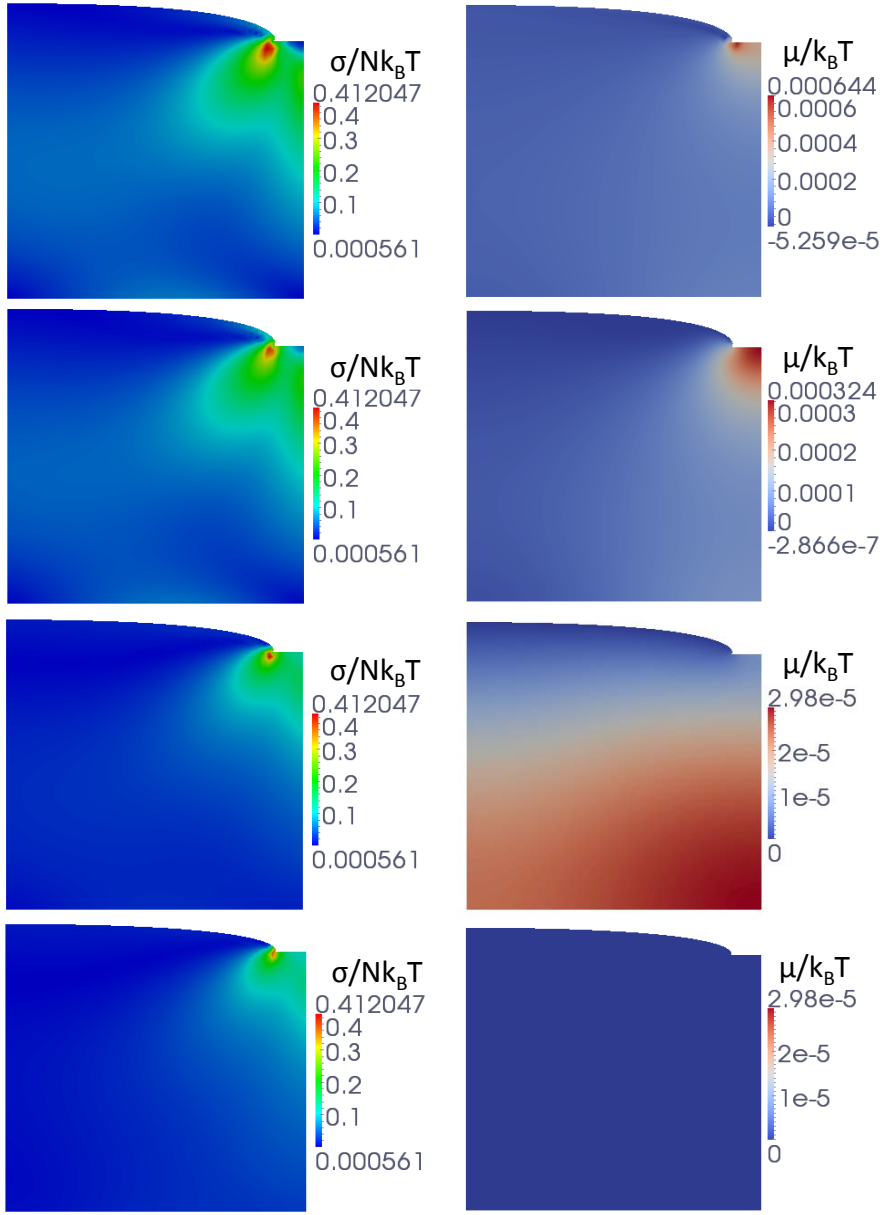

Fracture Properties of Hydrogels

- Reported values of fracture toughness range from 1 to 10000 J/m^2
- Fracture mechanism may vary over different types of hydrogels
- Potential rate dependence may relate to viscoelasticity or solvent diffusion
- Experimental methods to measure fracture properties of hydrogels are not well developed.

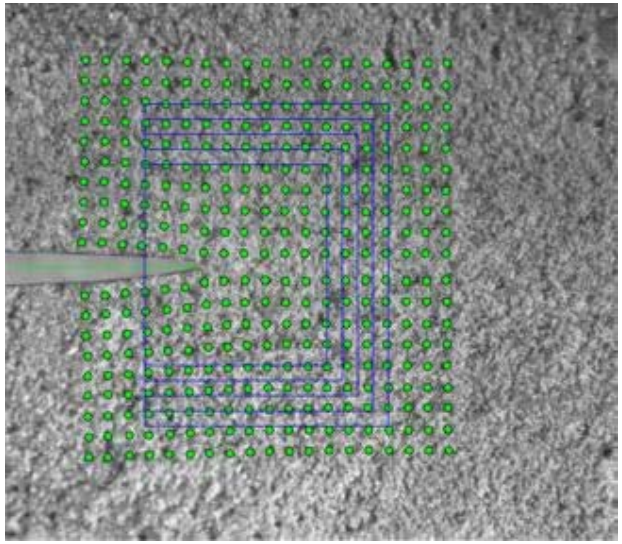

Kwon et al., 2011.

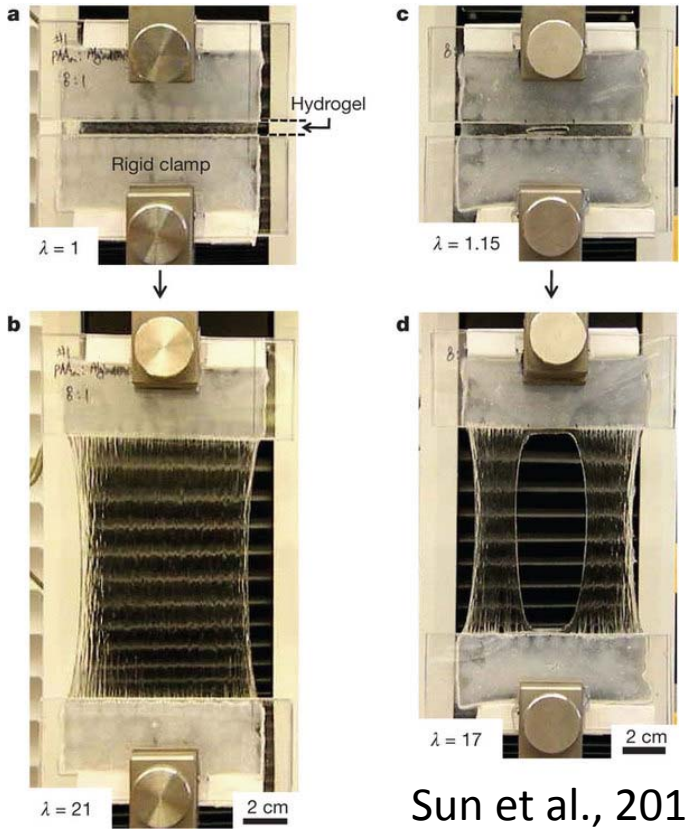

Sun et al., 2012.

A center crack model

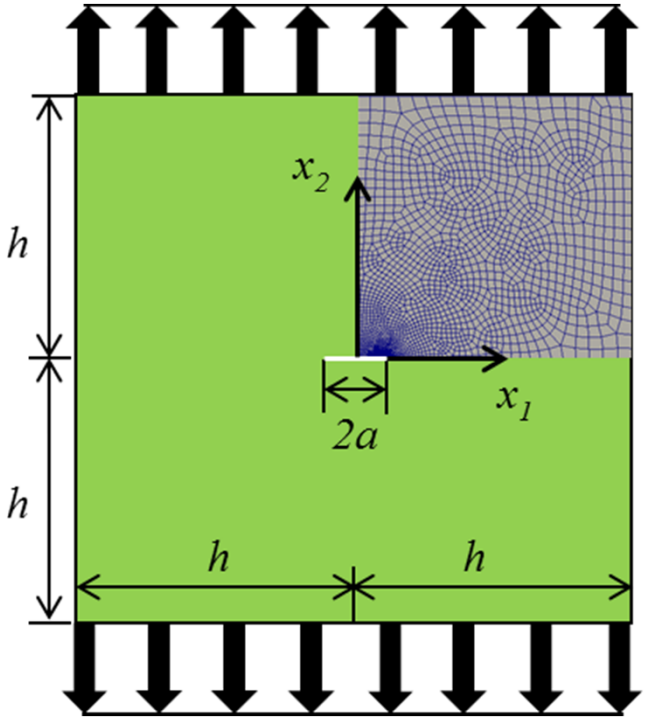

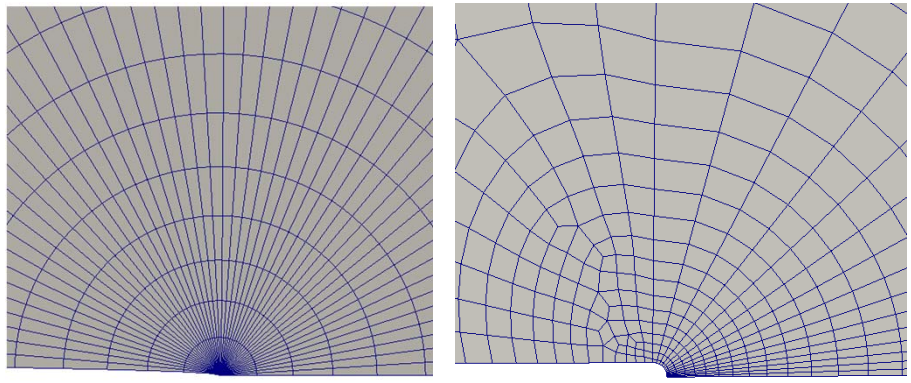

- Consider a center crack in a hydrogel plate under remote strain
- A nonlinear, transient finite element method is employed
- Sharp and notched crack geometries are used for small to large deformation

Bouklas et al., JAM 2015

Immersed and not-immersed cases

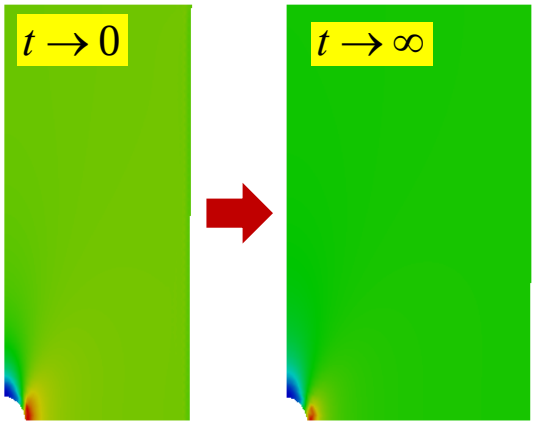

- Hydrogel is immersed in solvent
- Assume solvent-permeable boundaries and crack faces

$$\nu_0 = 0.5$$

$$\nu_\infty = \frac{1}{2} - \frac{N\Omega}{2}\left[\frac{1}{\lambda_0^2(\lambda_0^3 - 1)} + \frac{N\Omega}{\lambda_0^2} - \frac{2\chi}{\lambda_0^5}\right]^{-1}$$

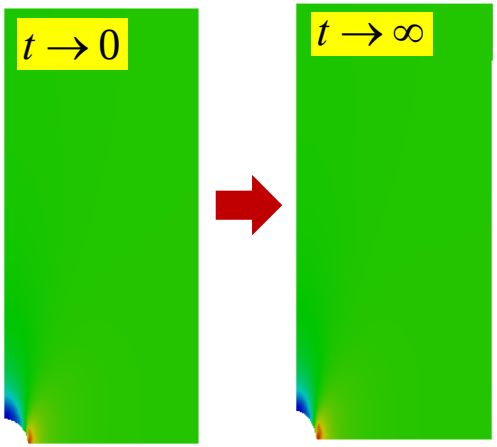

- Hydrogel is not immersed in solvent
- Assume solvent-impermeable boundaries and crack faces
- Overall volume is conserved, but solvent redistribution within the gel may lead to local volume change.

LEFM Predictions

Crack-tip stress field:

$$\sigma_{ij}(r,\theta) = \frac{K_I}{\sqrt{2\pi r}} f_{ij}^I(\theta) + T\delta_{1i}\delta_{1j}$$

$$K_I = \sigma_\infty \sqrt{\pi a} \qquad T = -\sigma_\infty$$

$$\sigma_\infty = \frac{2G\varepsilon_\infty}{1-\nu}$$

Stress would relax over time

$$G = \frac{Nk_BT}{\lambda_0}$$

Crack opening:

$$\hat{u}_2(x_1) = 2\varepsilon_\infty \sqrt{a^2 - x_1^2}$$

Crack opening would remain constant, independent of modulus or Poisson's ratio

Crack-tip stress fields

$\varepsilon_\infty = 10^{-3}$

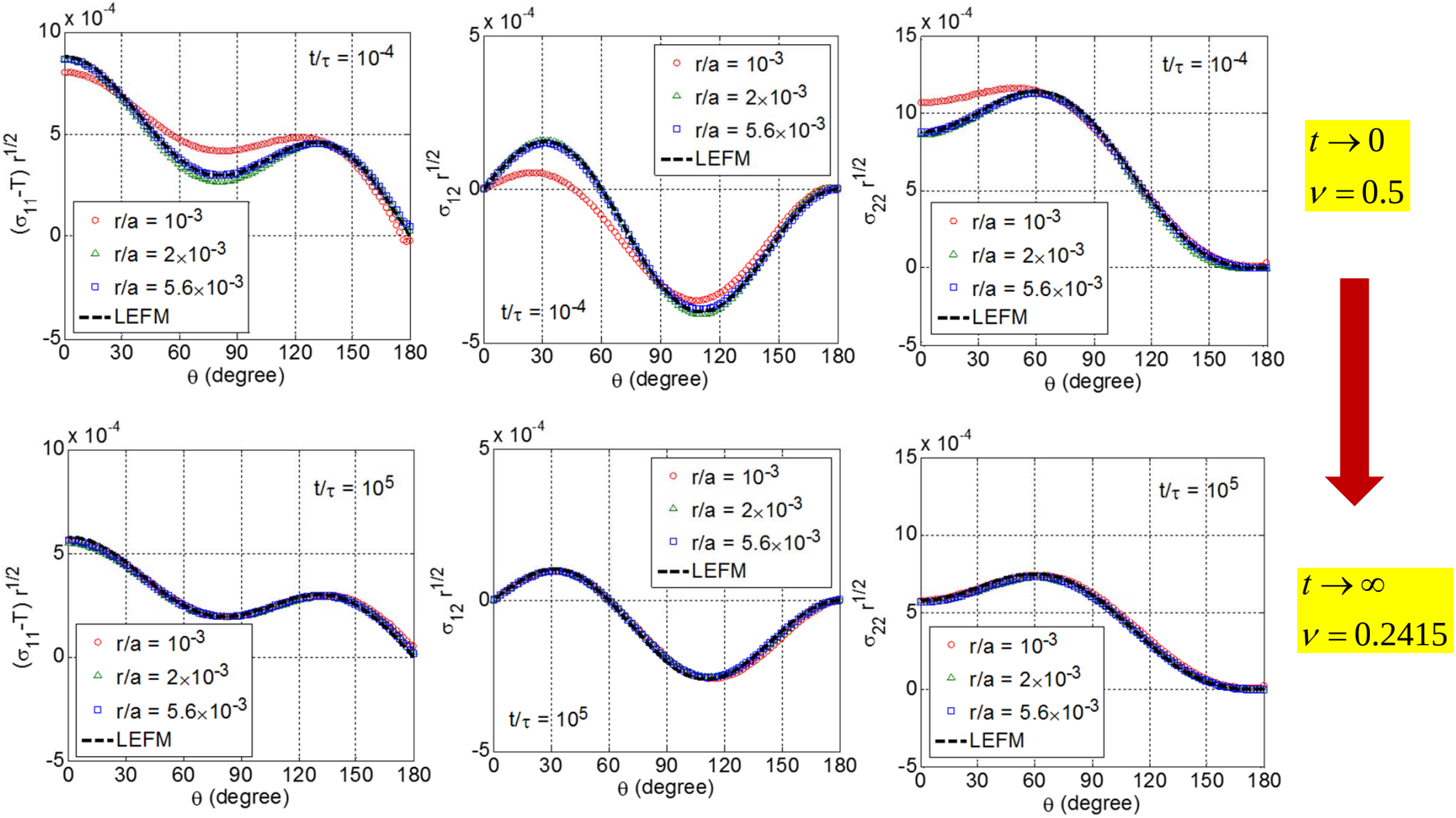

$t \to 0$

$\nu = 0.5$

$t \to \infty$

$\nu = 0.2415$

- The square-root singularity is maintained at both the instantaneous and equilibrium states, but the stress intensity factor is lower in the equilibrium state due to poroelastic relaxation.

Evolution of crack opening

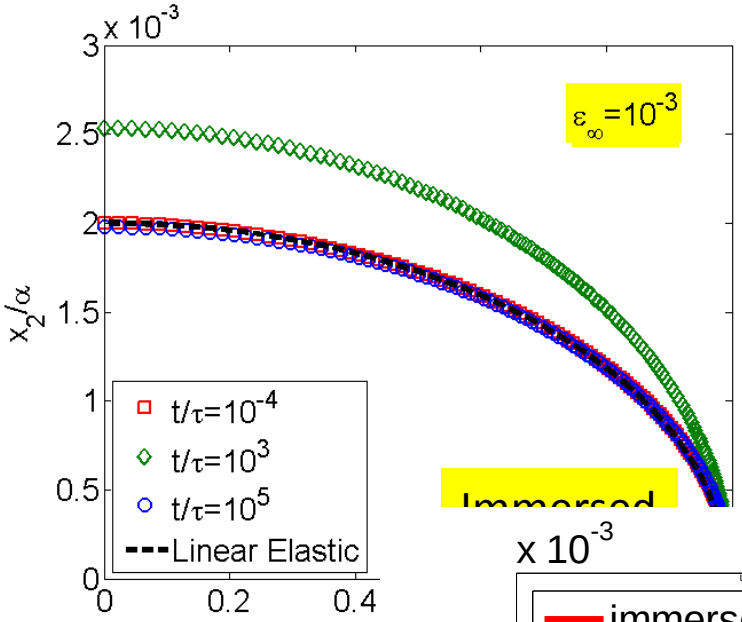

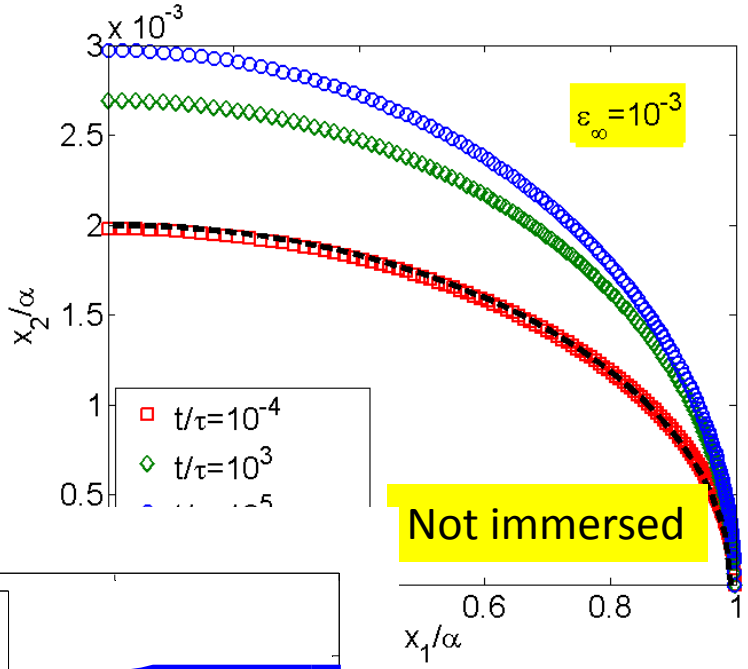

Opening at the center:

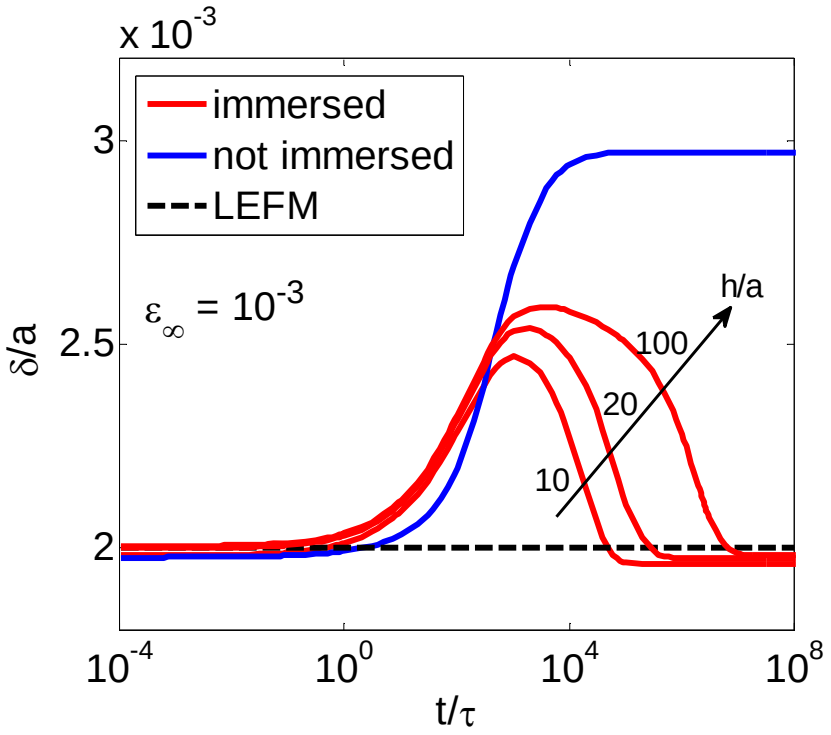

Bouklas et al., JAM 2015

Solvent diffusion around crack tip

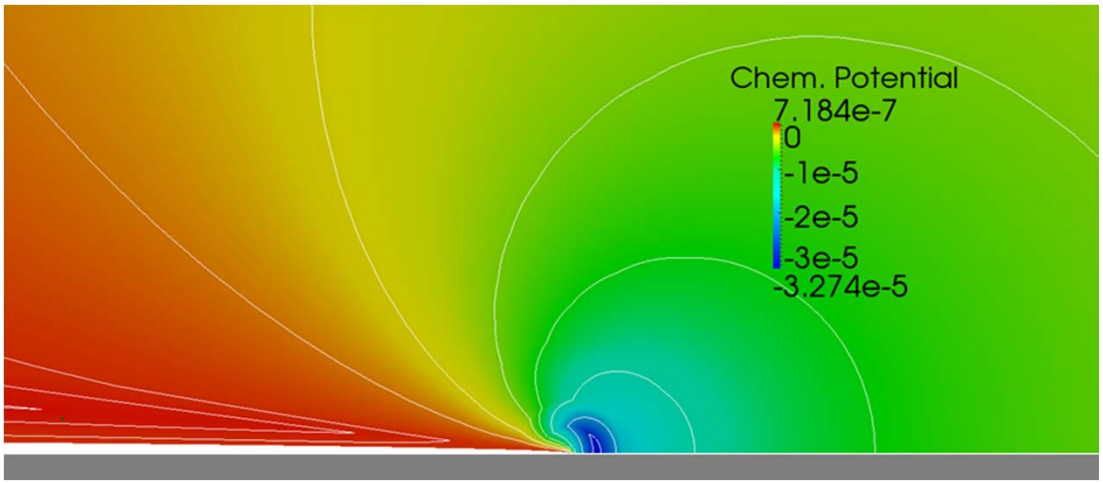

Instantaneous limit: Homogeneous solvent concentration, but *inhomogeneous* chemical potential.

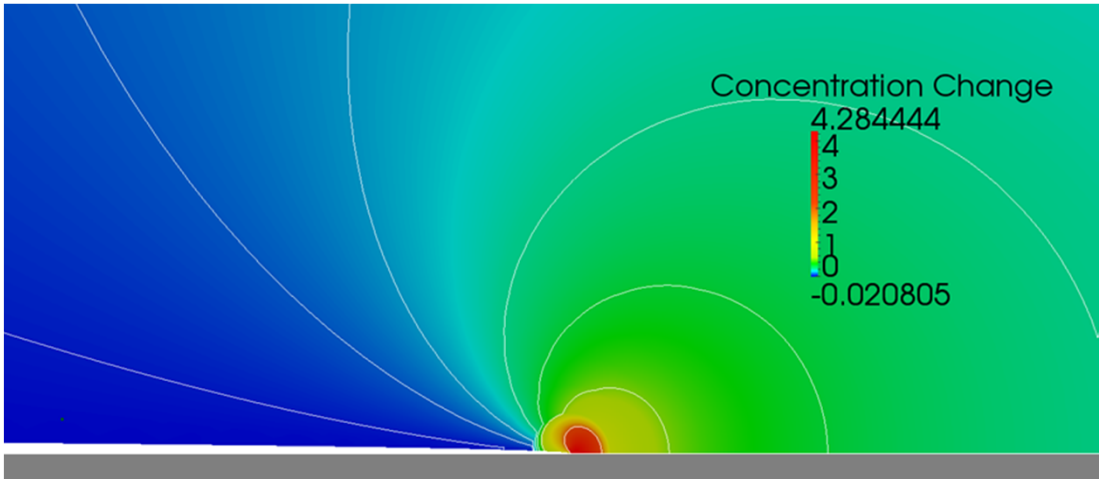

Equilibrium state: Homogeneous chemical potential, but *inhomogeneous* solvent concentration.

Bouklas et al., JAM 2015

Evolution of Solvent Concentration

- Immersed

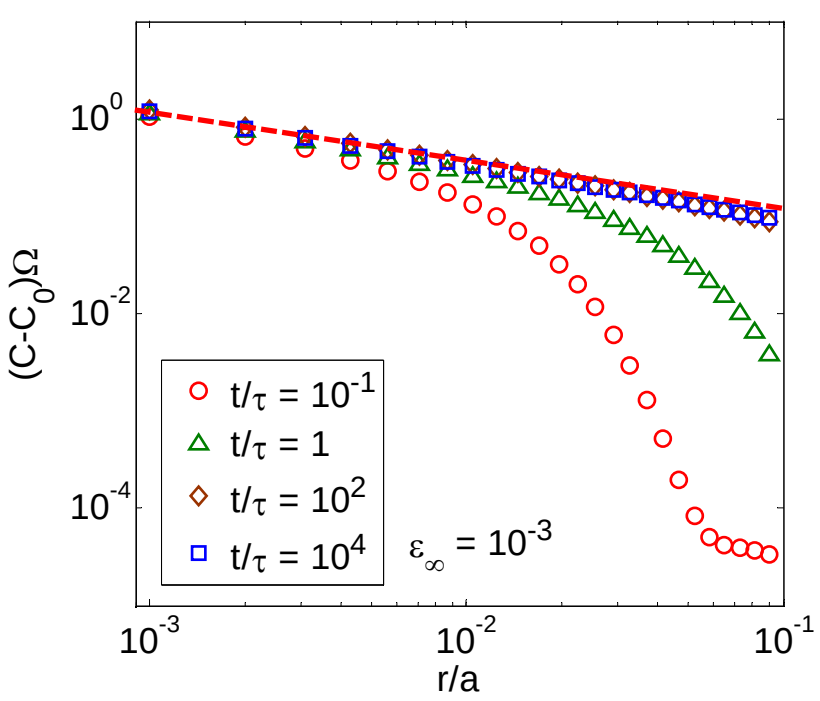

- Not-immersed

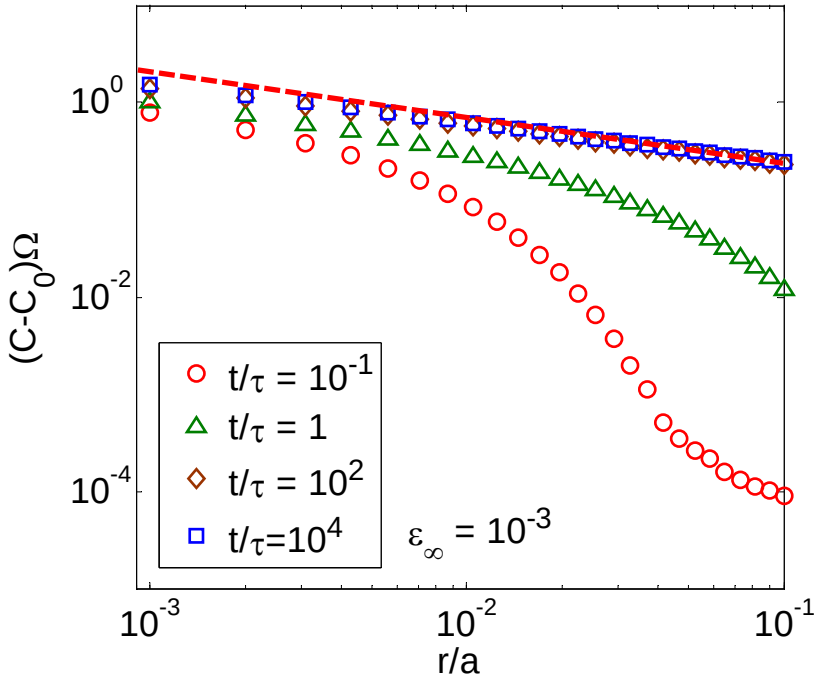

A singular concentration field is approached in the equilibrium state for both the immersed and not-immersed cases.

Bouklas et al., JAM 2015

Energy release rate

- Rate of change of potential energy:

$$\frac{d\Pi}{dt} = \int_{V_0} \frac{dU}{dt} dV - \int_{V_0} b_i \frac{dx_i}{dt} dV - \int_{S_0} T_i \frac{dx_i}{dt} dS - \int_{V_0} \mu r dV - \int_{S_0} \mu i dS$$

- Rate of dissipation due to diffusion:

$$\frac{d\Sigma}{dt} = -\int_{V_0} J_K \frac{\partial \mu}{\partial X_K} dV$$

- Total energy: $\Psi = \Pi + \Sigma$ $\quad \frac{d\Psi}{dt} = 0$

Conserved throughout the transient evolution (without crack growth).

- Rate of total energy change due to crack extension

$$\frac{d\Psi}{d\tilde{a}} = \int_{V_0} \left(\frac{dU}{d\tilde{a}} - \frac{\partial \mu}{\partial X_K} \frac{dI_K}{d\tilde{a}} \right) dV - \int_{S_0} \left(T_i \frac{dx_i}{d\tilde{a}} - \mu N_K \frac{dI_K}{d\tilde{a}} \right) dS$$

A modified J-integral

Define a nominal energy release rate: (per unit length of crack in the reference state)

$$J^* = -\frac{d\Psi}{d\tilde{a}}$$

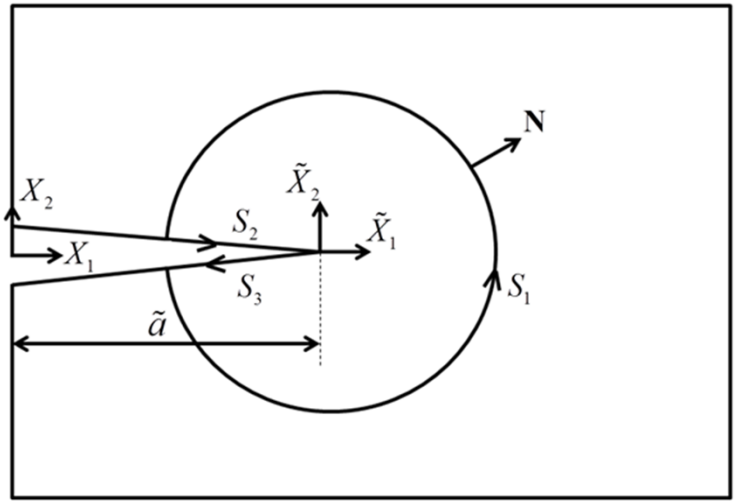

$$J^* = \int_{S_1} \left(UN_1 - s_{iJ} N_J \frac{\partial x_i}{\partial X_1} \right) dS - \int_{V_0} \mu \frac{\partial C}{\partial X_1} dV$$

$$J^* = \int_{S_1} \left(\hat{U}N_1 - s_{iJ} N_J \frac{\partial x_i}{\partial X_1} \right) dS + \int_{V_0} \frac{\partial \mu}{\partial X_1} C dV$$

- J* is path independent.
- The second form is more convenient for numerical calculations.
- A domain integral method is used to calculate J*.

Bouklas et al., JAM 2015

Evolution of J-integral

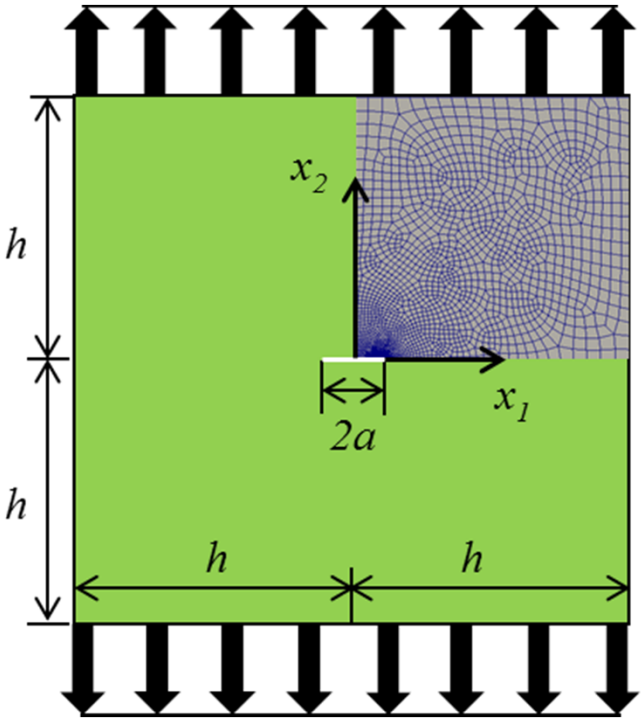

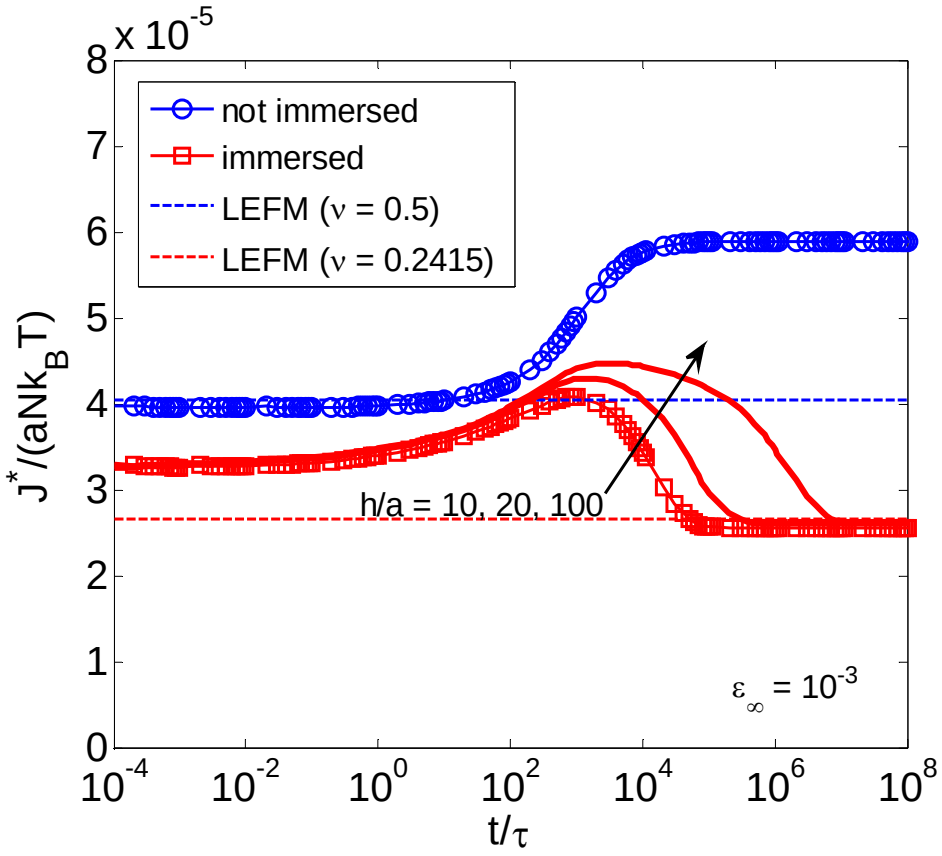

LEFM predictions at the instantaneous and equilibrium limits:

$$J^*(t \to 0) = 4\pi\lambda_0 N k_B T \varepsilon_\infty^2 a \qquad J^*(t \to \infty) = \frac{2\pi\lambda_0}{1-\nu_\infty} N k_B T \varepsilon_\infty^2 a$$

Dependence on material parameters

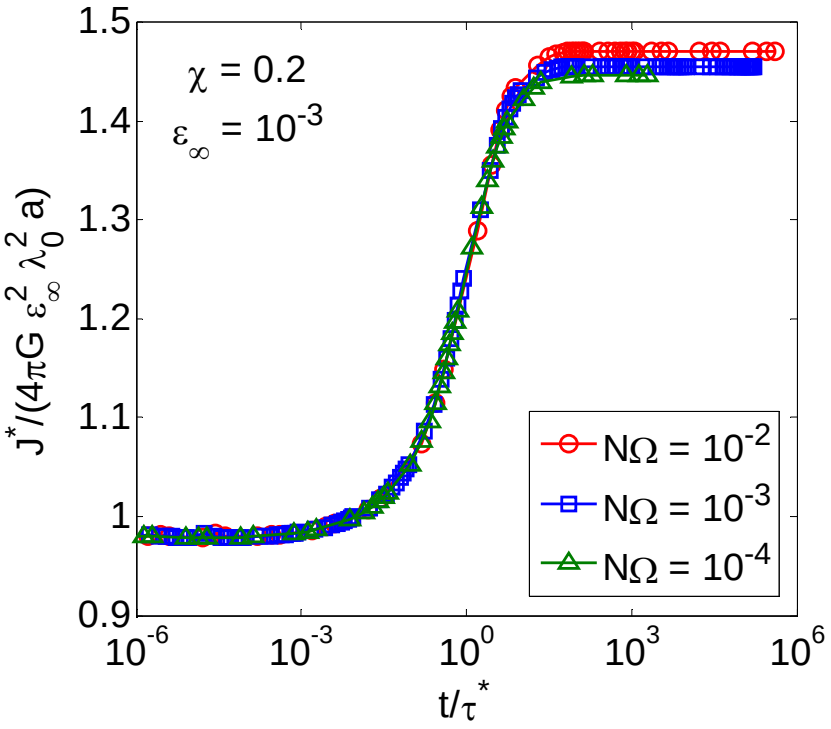

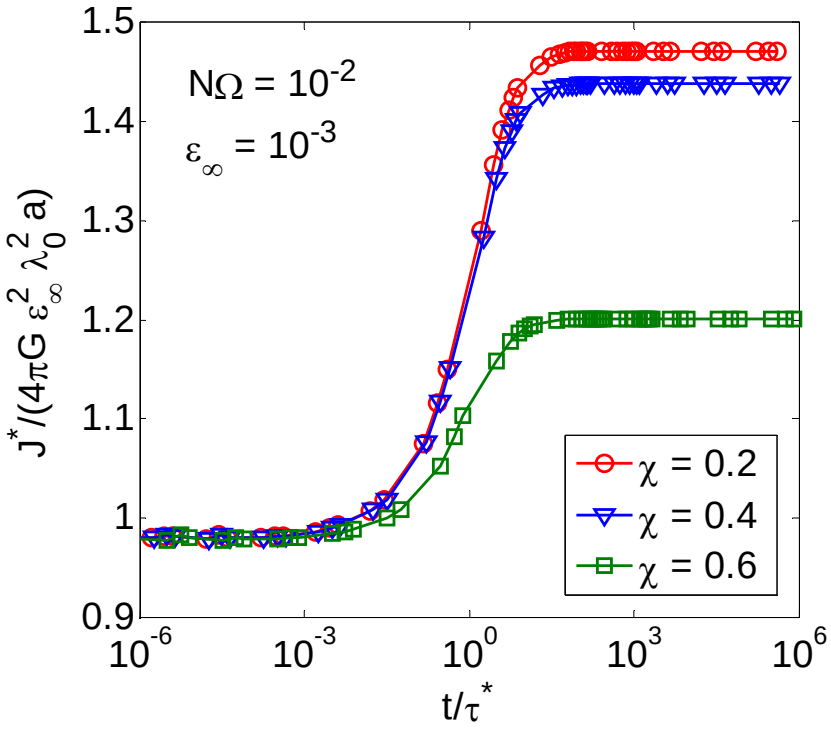

- The J* is well predicted by LEFM at the instantaneous limit (t → 0)
- The equilibrium J* depends sensitively on χ (good/poor solvent)
- The time scale is captured effectively by the poroelastic diffusivity
- Delayed fracture possible.

Bouklas et al., JAM 2015

Under moderately large remote strain

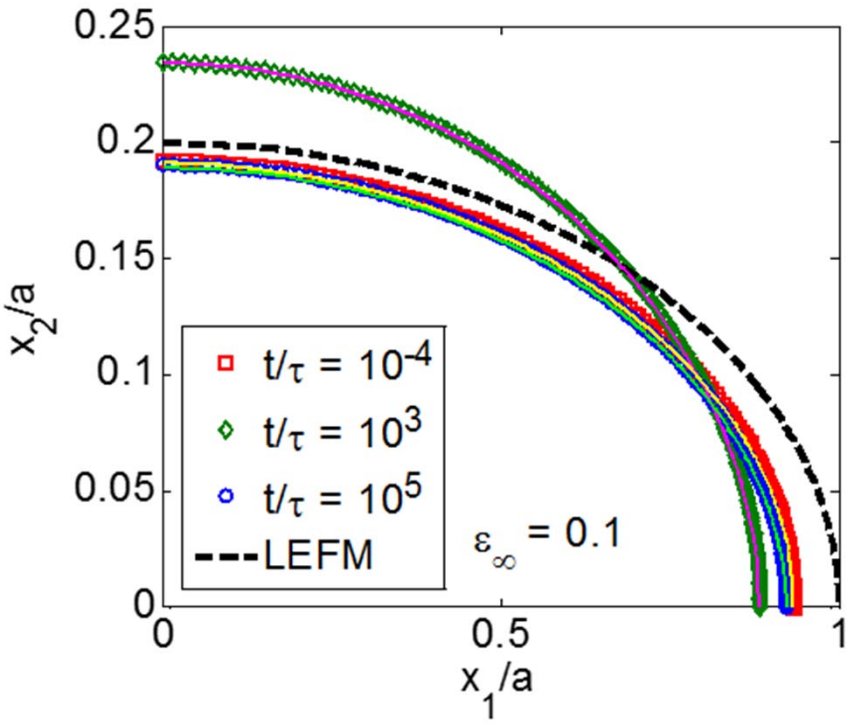

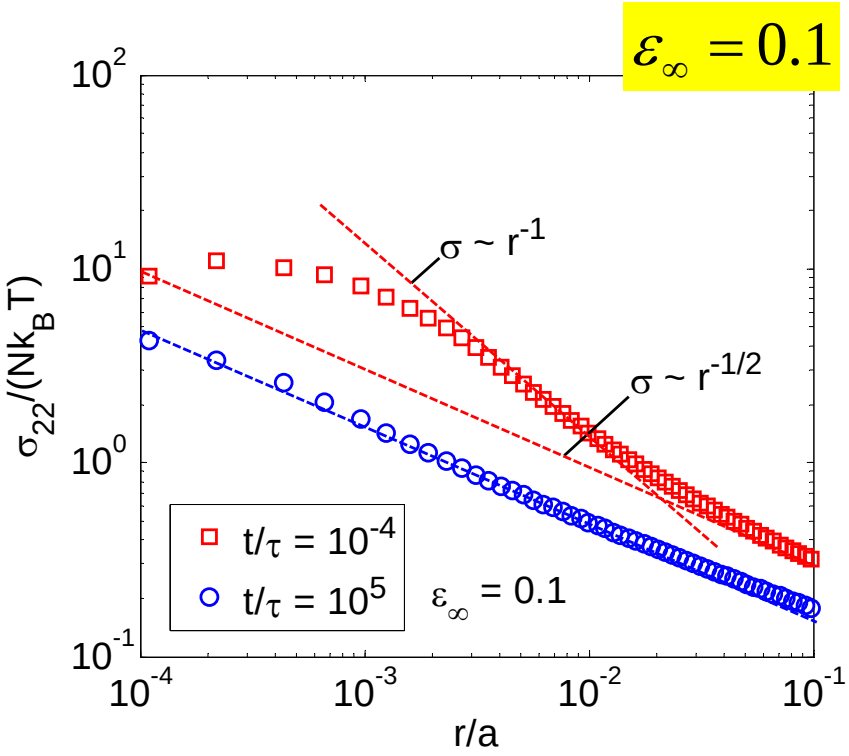

- Similar behavior for crack opening (and J* too, not shown)
- Stress distributions show transition of singularity: with a stronger 1/r singularity due to hyperelasticity and a weaker singularity closer to the crack tip due to solvent diffusion; the typical square-root singularity is approached at the equilibrium limit.

Bouklas et al., JAM 2015

Under large remote strain $\varepsilon_\infty = 0.5$

Immersed

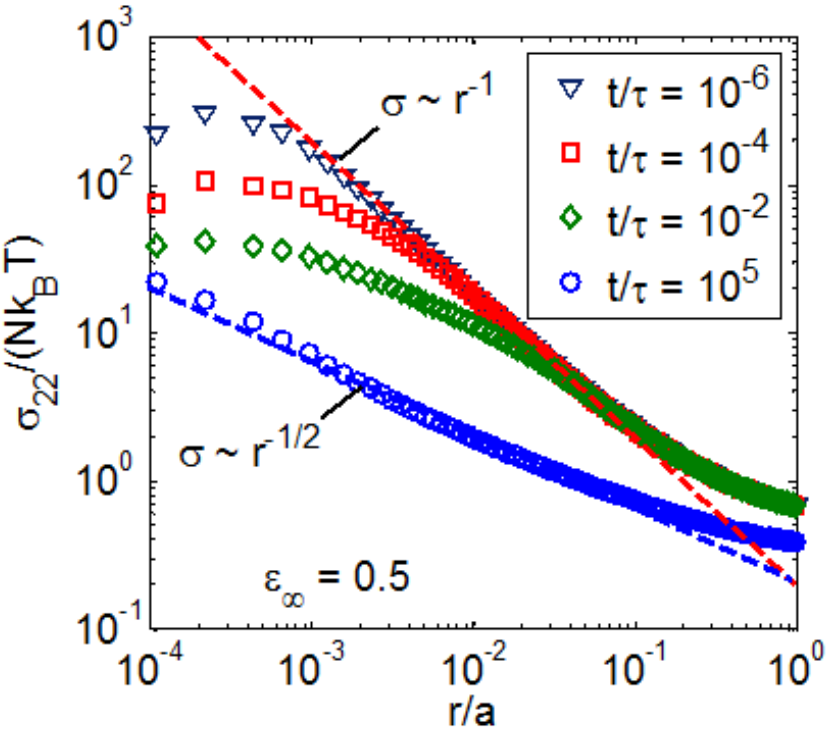

Not-immersed

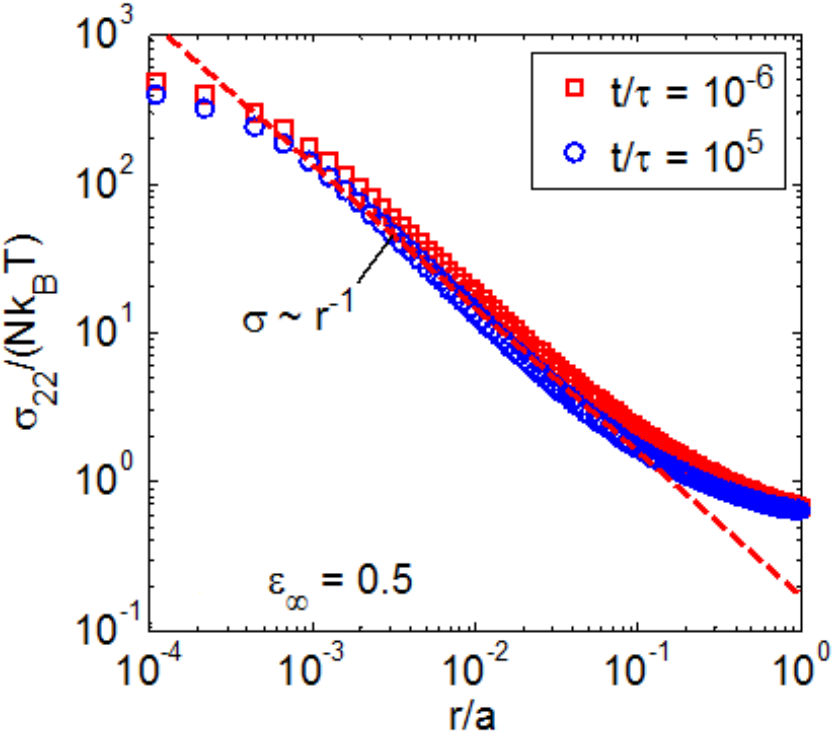

- The 1/r singularity becomes more prominent in both cases
- The singularity weakens over time for the immersed case

Bouklas et al., JAM 2015

J-integral

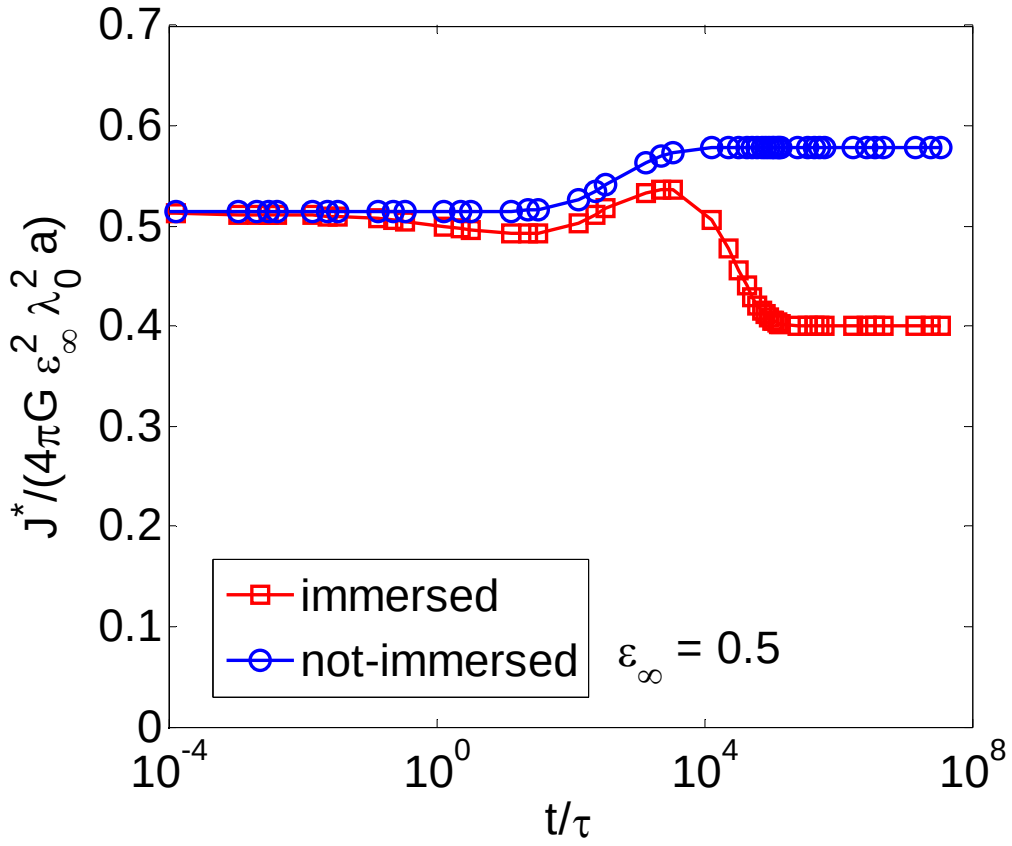

- The J* is considerably lower than the LEFM prediction, while the evolution trends are similar to the small-strain behaviors.

Bouklas et al., JAM 2015

Fracture Criterion

$$J^*(t) = J_c^*(?)$$

- The right hand side of the fracture criterion has to be determined by well-designed experiments.
- Could the right-hand side depend on time due to the evolving, inhomogeneous field of solvent concentration around the crack tip?

Summary

- A nonlinear, transient finite element method was implemented for large deformation of hydrogels coupled with solvent diffusion.
- The transient processes of constrained swelling (with surface instability) and flat punch indentation were studied in some details.
- Effects of solvent diffusion on the crack-tip fields and driving force for fracture of hydrogels were studied. A path-independent, modified J-integral was derived as the transient energy release rate of crack growth in hydrogels, although a complete fracture criterion is yet to be established.

Acknowledgments

- Min-Kyoo Kang
- Nikolas Bouklas
- Zhigen Wu
- Chad Landis

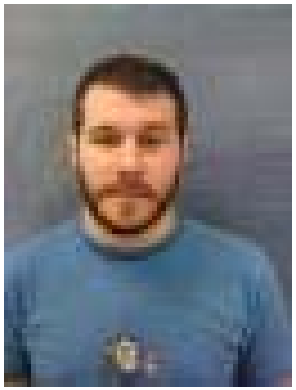

- Funding by NSF